frontiers | Frontiers in Membrane Science and Technology

TYPE Original Research
PUBLISHED 16 December 2025
DOI 10.3389/frmst.2025.1727515

OPEN ACCESS

EDITED BY
Yunxia Hu,
Tianjin Polytechnic University, China

REVIEWED BY
Asim Laeeq Khan,
COMSATS University Islamabad, Pakistan
Gaoxiang Zhang,
Lishui University, China

*CORRESPONDENCE
S. Ranil Wickramasinghe,
swickram@uark.edu

RECEIVED 17 October 2025
REVISED 26 November 2025
ACCEPTED 28 November 2025
PUBLISHED 16 December 2025

CITATION
McKean T, Wilmoth C, Wickramasinghe SR and Hestekin J (2025) Membrane adsorbers for low-pressure metal ion capture.
Front. Membr. Sci. Technol. 4:1727515.
doi: 10.3389/frmst.2025.1727515

Membrane adsorbers for low-pressure metal ion capture

Thomas McKean, Courtney Wilmoth, S. Ranil Wickramasinghe* and Jamie Hestekin

Ralph E. Martin Department of Chemical Engineering, University of Arkansas, Fayetteville, AR, United States

Heavy metal ions are notoriously difficult to remove from water systems without the infrastructure present at a drinking water treatment plant. This work aimed to develop membrane adsorbers capable of capturing heavy metals at low pressure to avoid the need for extensive infrastructure. Removal of copper as a representative heavy metal was investigated. Membrane adsorbers were fabricated by using photo-initiated radical polymerization to graft glycidyl methacrylate (GMA) from the surface of polyethersulfone microfiltration membranes. The GMA modified membrane was sulfonated through an epoxide ring opening reaction to introduce sulfonic acid groups. The effect of grafting time and temperature on the degree of grafting and membrane performance (permeability and adsorption capacity) were determined. The reactions conditions that provided best performance were 4 min UV exposure at 35 °C. Under these conditions, the degree of grafting was 9% while maintaining a low operating pressure of 0.1 bar. Five and 6 min of UV exposure time increased the DOG to 19% and 41%, respectively, but compromised low pressure operation. Membrane surface properties were characterized by Fourier transform infrared spectroscopy and scanning electron microscopy. Membrane performance was investigated by determining membrane permeability and static and dynamic capacity. The dynamic binding capacity was 64.05 ± 0.6 mg Cu/g grafted weight. Using membranes in series demonstrated linear scaleup. Further at a flux of 135 $Lm^{-2}h^{-1}$ the feed pressure was under 0.15 bar ensuring low pressure operation. These results highlight the potential of membrane adsorbers for low pressure removal of heavy metals.

KEYWORDS

membrane adsorber, heavy metal, low pressure, radical polymerization, water treatment

1 Introduction

The toxicity of heavy metal ions to humans, animal and plant life has been thoroughly documented over recent years. Metals including arsenic, lead, chromium, cadmium, mercury, copper, zinc, and others can lead to numerous health problems, including damage to organs, nervous systems, reproductive systems, and carcinogenicity (Jaishankar et al., 2014). Contamination of water sources by these heavy metals through wastewater discharge, mining activities, runoff, and aging infrastructure has led to increased risk of exposure to these toxic compounds and a loss of otherwise potable water sources worldwide (Razzak et al., 2022). Furthermore, the infrastructure necessary to treat water contaminated with heavy metals through methods such as reverse osmosis, chemical precipitation, electrical-based, or catalytic methods cannot be implemented in remote or rural areas based on size and economic limitations (Agarwal et al., 2020). Adsorptive technologies are promising for removal of heavy metals without highly developed

infrastructure. Activated carbon is a common adsorbent. However, it can suffer from issues related to sensitivity to operating conditions, variability based on production method, and difficulty to regenerate. Newer materials include biomaterials and nanomaterials which are currently expensive to produce and often cannot operate at high throughput (Neolaka et al., 2023; Albqmi et al., 2023).

Membrane technologies are attractive for capturing heavy metals from water based on their ability to remove heavy metals, reliability, lack of harmful byproducts, potential for low-energy separation, reusability, and easy process integration (Xiang et al., 2022). Reverse osmosis (RO) membranes are known for their excellent rejection of heavy metals (Ozaki et al., 2002; Petrinic et al., 2015). Nanofiltration (NF) membranes also have varying degrees of success rejecting divalent or trivalent heavy metals (Wanjiya et al., 2024; Nompumelelo et al., 2023). Ultrafiltration (UF) membranes commonly contain pores larger than the size of heavy metal ions even when hydrated and as such cannot reject heavy metals as effectively (Chitpong and Husson, 2017a). Enhancements to UF membranes such as the addition of micelles or polyelectrolytes have been studied to increase heavy metal removal (Huang et al., 2010; Ennigrou et al., 2009). However even for ultrafiltration, feed pressures up to 3 bar may be required. These operating pressures typically need to be supported by significant infrastructure, leading to significant capital cost, operating cost, and process footprint which could be problematic in rural areas. Membrane adsorbers on the other hand operate at pressure well below 1 bar.

Membrane adsorbers are a possible alternative to NF and RO typically used to remove heavy metal ions from wastewater and drinking water (Chitpong and Husson, 2017a; Sepesy et al., 2022; Chitpong and Husson, 2017b). Adsorptive membranes combine the effective removal of heavy metals provided by adsorption mechanisms with the potential for high-throughput operation and other advantages of membrane technologies. Membrane adsorbers capture heavy metal ions through chelation or ion exchange rather than the size exclusion mechanisms used by NF and RO membranes. Research has focused on modification of the base polymer used to form the membrane to include the adsorptive ligands. Metal recovery applications typically employ peptides or amino acids that are highly selective for specific metals of interest (Johnson and Duval, 2025). Toxic metals can be removed through chelation with amine groups or either ion exchange or chelation using highly negatively charged acids (Sepesy et al., 2022; Sokker et al., 2009). A variety of strategies to introduce these ligands to the membrane structure have been investigated including synthesizing negatively charged polymers (Fraser et al., 2022), blending (Khodabakhshi and Goodarzi, 2021), layer-by-layer synthesis (Pei et al., 2021), modification of the membrane polymer prior to casting (Vatanpour et al., 2022; Wang et al., 2016), and modification of the membrane polymer post casting (Chitpong and Husson, 2017b). The chemical functionalization process allows for strong control over the resulting membrane properties, adsorption capacity and flux.

A common approach is to graft glycidyl methacrylate (GMA) from the membrane surface given its ease of attachment and the ability to further modify the terminal epoxide group (Yune et al., 2012). GMA can be grafted to different polymers through a variety of different methods including photo-induced radical polymerization onto polyethersulfone (Yu et al., 2020), atom transfer radical polymerization onto polyvinylidene fluoride (Johnson and Duval, 2025), and radiation-induced grafting onto cellulose and polypropylene (Sokker et al., 2009; Bondar et al., 2004). Of these techniques, photo-induced radical polymerization stands out for its speed and simplicity. Another approach is to form a mixed matrix composite membrane combining adsorptive nanomaterials such as metal oxides (Garcia-Chirino et al., 2025), zeolites (Akale and Shaikh, 2024) graphene oxide (Mukherje et al., 2016), or metal organic frameworks (Escamilla et al., 2024), with the base polymer. However, current industrial research favors covalently functionalized ligands given issues related to aggregation, cost, and leaching suffered by nanomaterials in these applications.

The goal of this work was to develop membrane adsorbers functionalized with sulfonic acid groups capable of removing heavy metal ions from water at low pressure. Copper (II) was chosen as the heavy metal of interest due to its toxicity, prevalence in areas difficult to access with water treatment plants such as areas with high mining activity, and increased risk of contamination in the future given increasing levels of electronics manufacturing (Soon et al., 2024). Copper concentrations in excess of 100 ppm have been detected in wastewaters (Liu et al., 2023). On the other hand, the EPA limit is 1.3 ppm in drinking water (U.S. Environmental Protection Agency, 2025). Studies have also demonstrated adsorption behavior for Cu^{2+} is similar to other divalent heavy metal ions such as Pb^{2+} and Ni^{2+}, suggesting that copper removal data can translate to the removal of other heavy metals from water (Jasim and Ajjam, 2024; Mohammed and Mahmood, 2023). Sulfonic acid was chosen as the adsorption ligand due to its highly negative charge (pKa = −6). It has successfully been used to functionalize the surface of adsorbents for heavy metal ion removal through a combination of electrostatic, ion exchange, and chelation mechanisms (Fraser et al., 2022; Bondar et al., 2004; Liang and Zou, 2020). This work sought to extend this principle to membranes given membrane adsorbers are capable of much higher throughput processing. This approach also addresses a gap in literature since most work focused on membrane adsorbers for metal adsorption has focused on chelation with amines, amino acids, or peptides.

Sulfonic acid was introduced to the membrane surface through a two-step process where GMA was first grafted from the membrane through photo-initiated radical polymerization. This was followed by addition of sulfonic acid through an epoxide ring opening reaction. Modified membranes were characterized by determining the degree of grafting (DOG) and scanning electron microscopy (SEM) imaging of the surface. Membrane permeability and static and dynamic capacities for copper were determined for a range of modification times. The ease of scale up was explored by testing three membranes in series.

2 Materials and methods

2.1 Materials

Hydrophilized polyethersulfone (PES) microfiltration membranes, pore size of 0.22 μm, were purchased from MilliporeSigma (Burlington, MA, United States) and washed with water and ethanol and dried under vacuum prior to use. Ethanol (Decon Labs, King of Prussia, PA, United States, 99%), butanol (Thermo Fischer Scientific, Waltham, MA, United States, 99%), and glycidyl methacrylate (MilliporeSigma, Burlington, MA, United States, 97%) were used as obtained during the grafting

process. Isopropyl alcohol (MilliporeSigma, 70%) and sodium sulfite (Thermo Fischer Scientific) were used during the functionalization reaction. Copper (II) nitrate (Ward's Science, Rochester, NY, United States) was used for adsorption studies.

2.2 Membrane modification

Figure 1 shows the reaction scheme used to functionalize the membranes with sulfonic acid. The base PES membranes were initially washed in DI water and dried in a vacuum oven. Next they were soaked in the reaction solution consisting of 20% ethanol, 20% butanol, and 5% GMA in water and placed inside a UV reactor (Honle UV Technologies, Gilching, Germany) and exposed to high intensity UV light (4.25 mW/cm^2) for 1–6 min at different temperatures. After the reaction, the membranes were washed with ethanol to remove unreacted monomer followed by washing with water and drying under vacuum. The DOG was determined using Equation 1, where w_1 is the weight of the membrane after grafting and w_0 is the weight of the membrane after initial washing and drying.

$$DOG = \frac{w_1 - w_0}{w_0} \tag{1}$$

The GMA modified membranes were placed in a solution of 15% isopropyl alcohol and 10% sodium sulfite in water at 80 °C for 2.5 h. The membranes were then placed in a solution of 0.5 M sulfuric acid for 2 h. Sulfonic acid was added via an acid-catalyzed ring-opening reaction (Sokker et al., 2009).

During surface modification grafting will occur not just on the outer membrane surface but also in the membrane pores (Car et al., 2018). Grafting in the membrane pores will lead to pore constriction and ultimately blocking which will reduce membrane permeability. DI water permeability was measured at a flow rate of 20 mL/min using a peristaltic pump. The resulting pressure and any drop in flow rate due to changes in the membrane permeability were recorded. Pressure was monitored using a pressure gauge and the flow rate was calculated by weighing the permeate collected over a certain amount of time. The membranes were mounted in holders from Advantec (Cole-Parmer, Court Vernon Hills, IL, United States) with an area of 17.35 cm^2. Permeability was calculated using Equation 2. Where P is permeability, (L m^{-2} h^{-1} bar^{-1}), V permeate volume (L), A membrane area (m^2), t is time (h), and p is pressure (bar).

$$P = \frac{L}{m \times t \times p} \tag{2}$$

Fourier transform infrared (FTIR) spectroscopy (SHIMADZU QATR, Shimadzu, Columbia, MD, United States) was used to determine changes in surface chemical groups as a result of surface modification. Scanning electron microscopy (SEM) (FEI XL-30, Phillips, Cambridge, MA, United States) was used to determine change in surface pore structure due to surface modification.

2.3 Static binding experiments

The effect of GMA grafting time on the static binding capacity of copper was determined. The membranes were submerged in solutions of different concentrations of copper (II) nitrate and left under shaking for 24 h. The copper concentration in solution was determined using inductively coupled plasma mass spectroscopy (Thermo iCAP Q, Thermo Fischer, Waltham, MA, United States). At least three membranes were tested for each data point. The amount of copper adsorbed onto the membrane at equilibrium per increase in weight of the membrane due to grafting (grafted weight) was calculated using Equation 3.

$$q_e = \frac{(C_0 - C_e)V}{m} \tag{3}$$

q_e (mg/g) is the weight of adsorbed copper at equilibrium per membrane weight, C_0 is the initial concentration, and C_e is the equilibrium concentration of copper ions in solution, V is the solution volume, and m is the grafted weight (g). The maximum adsorption capacity was determined at equilibrium through Equation 4 (Vatanpour et al., 2022).

$$K = \frac{q_e}{C_e[Q - q_e]} \tag{4}$$

where Q (mg/g) is the maximum adsorption capacity and K (L/mg) is the adsorption affinity. Equation 4 was linearized to give Equation 5.

$$\frac{C_e}{q_e} = \left[\frac{1}{Q}\right]C_e + \left[\frac{1}{QK_L}\right] \tag{5}$$

By rearranging Equation 4 as follows

$$q_e = \frac{QC_e}{\frac{1}{K} + C_e} \tag{6}$$

K, the adsorption capacity is the reciprocal of the concentration at which 50% of the binding sites are utilized.

2.4 Filtration experiments

Solutions of different copper concentration were filtered using membranes grafted for 4 min at a flux of 135 Lm^{-2}h^{-1}. The membrane with 4 min grafting time was chosen based on the permeability results. Further the flux of 135 Lm^{-2} h^{-1} was chosen to be higher than or comparable to the operating flux of UF membranes while operating at a much lower pressure. UF membranes are often operated between 50 and 100 Lm^{-2} h^{-1} at pressures between 1 and 3 bar, compared to 135 Lm^{-2} h^{-1} at 0.07 bar in this work (Barakat and Schmidt, 2010). Samples were collected over time to create breakthrough curves used to determine the maximum dynamic binding capacity. Dynamic capacity was determined through integration of the obtained breakthrough curve. At least three membranes were tested for each concentration. After single membrane filtration, membranes in series experiments were conducted by stacking 3 membranes in series and repeating the analysis (see Figure 2).

3 Results and discussion

3.1 Membrane characterizations

The effect of grafting temperature and time on DOG were determined. Figure 3A shows the change in DOG as a function of temperature at a constant grafting time of 5 min. The maximum

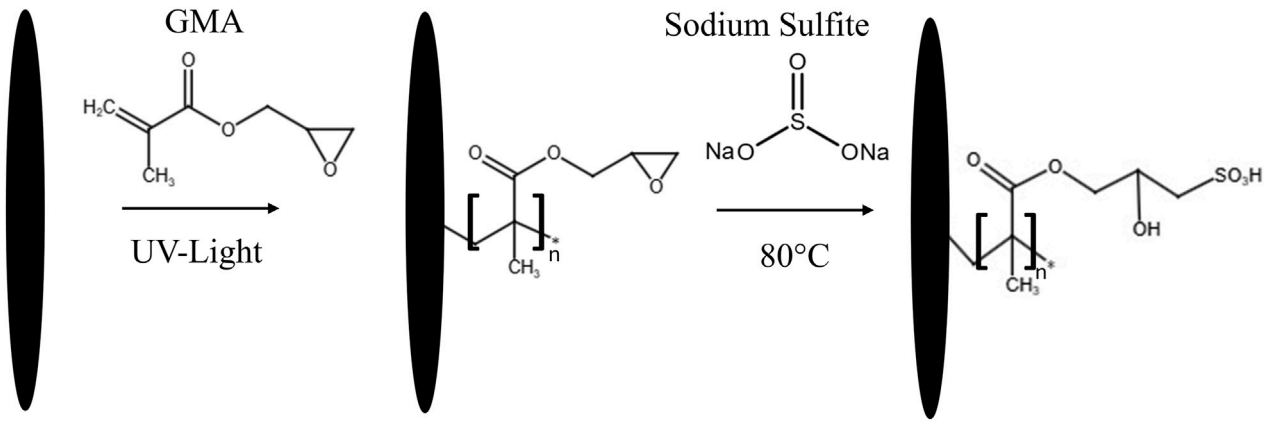

FIGURE 1
Reaction scheme for membrane functionalization. GMA was first grafted from the surface of the PES membrane followed by acid catalyzed epoxy ring opening to add sulfonic acid groups.

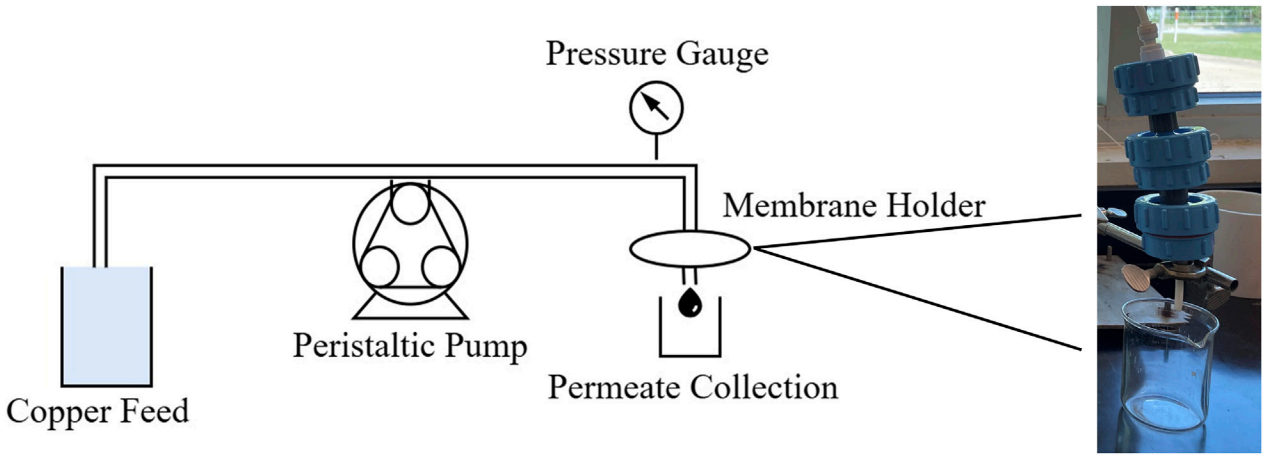

FIGURE 2
Schematic of membrane testing setup for determining membrane permeability. Membrane holders stacked in series are also shown.

temperature tested was 35 °C in order to ensure stability of the membrane. It was observed that increasing the temperature had a strong impact on the DOG. From these results, 35 °C was chosen as the constant grafting temperature for subsequent experiments. Next, UV grafting time was varied from 1 to 6 min, and the resulting DOG is presented in Figure 3B. As can be seen grafting times less than 3 min led to little grafting.

Based on these results, 1 min grafting time was not considered further as there was little change in DOG. IR spectra for the base membrane, after GMA grafting and sulfonic acid functionalization are shown in Figure 4 for a 4 min grafting time. A new peak at 1725 cm^{-1} characteristic of the C=O carbonyl group stretching appears after GMA grafting (Yu et al., 2020). After sulfonic acid functionalization a new peak appears at 1030 cm^{-1} characteristic of the sulfonic group (Fraser et al., 2022). Appearance of these new peaks confirmed successful membrane modification. Studies were also performed to examine the growth of these characteristic peaks with grafting time. Figure 5A shows the growth of the carbonyl peak characteristic of GMA with increasing grafting time. As can be seen a 2 min grafting time shows no carbonyl peak. Consequently sulfonation was not conducted for this membrane. Figure 5B shows the growth of the sulfonate peak with increasing GMA grafting time and hence increasing density of epoxide groups. Further, stability of the membranes in an acidic environment was confirmed after the reaction in sulfuric acid at 80 °C as no change in the spectrum was observed (Figure 4).

DI water permeability measurements were conducted for membranes with different UV grafting times. The results are presented in Figure 6. The unmodified membrane reached a pressure of 0.069 bar. Based on the DOG and spectroscopy data (Figures 3B, 5) grafting times of 1 and 2 min were not investigated. For 4 min grafting time the average pressure was 0.090 ± 0.014 bar, for a 5 min grafting time the average pressure was 1.656 ± 0.069 bar and for a 6 min the pressure was 1.931 ± 0.241 bar. The results in Figure 6 indicate that grafting times greater than 4 min led to very low permeabilities similar to UF membranes. Further the required feed pressure is much higher. Results for 3 min grafting time are not

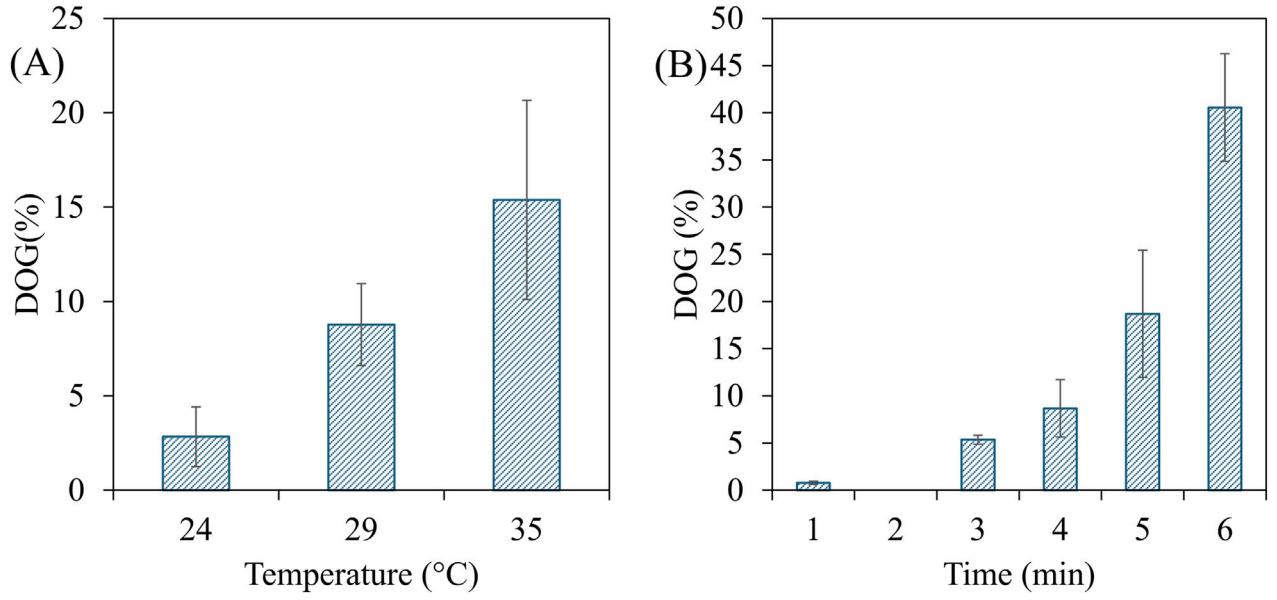

FIGURE 3
DOG as a function of **(A)** temperature and **(B)** grafting time.

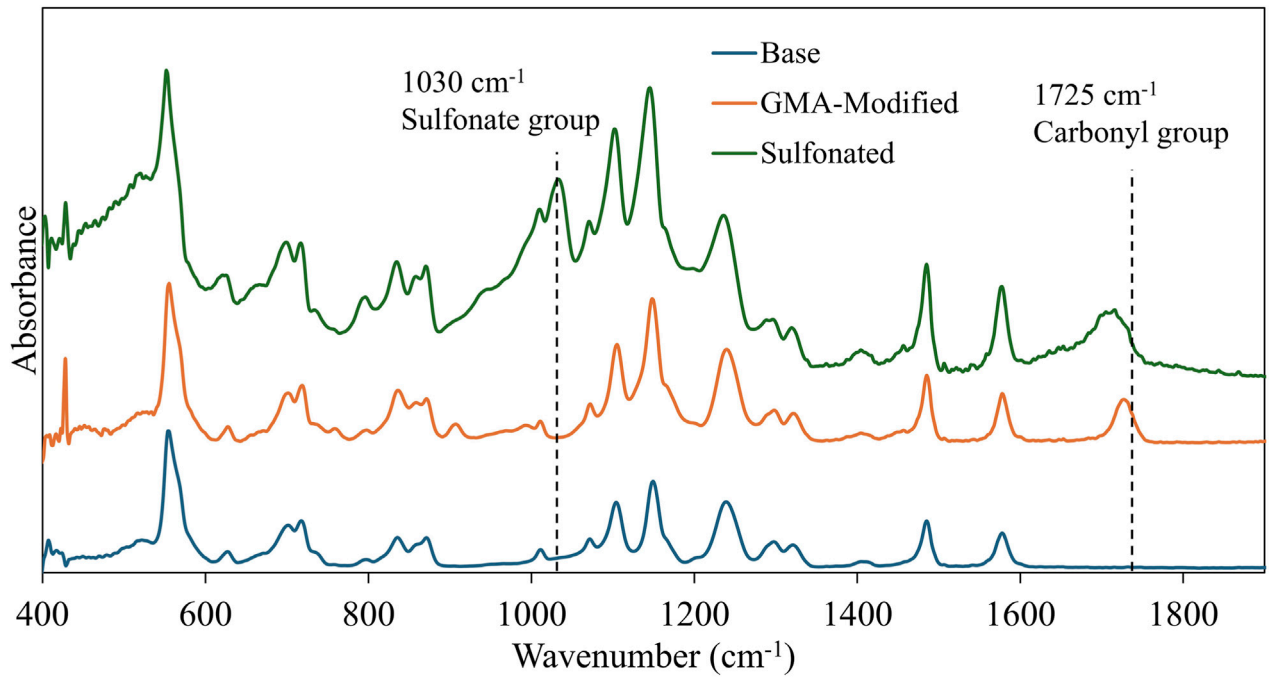

FIGURE 4
FTIR spectra for base, GMA-grafted, and sulfonated PES membranes for 4 min grafting time.

included as the DOG is much less than 4 min (see Figure 3B), yet the feed pressure for 4 min is low, being less than 0.1 bar.

SEM images of the membrane surface (Figure 7) for the base, 4, 5, and 6-min grafting time membranes indicate that as the grafting time increases, the membrane structure clearly changes due to an increasing amount of grafted material on the membrane surface.

3.2 Static capacity experiments

Static capacity experiments were conducted for membranes grafted for 4 and 6 min (Figure 8). The permeability data (Figure 6) combined with SEM images (Figure 7) indicate that 4 min is likely the optimal grafting time. Lower grafting times led to

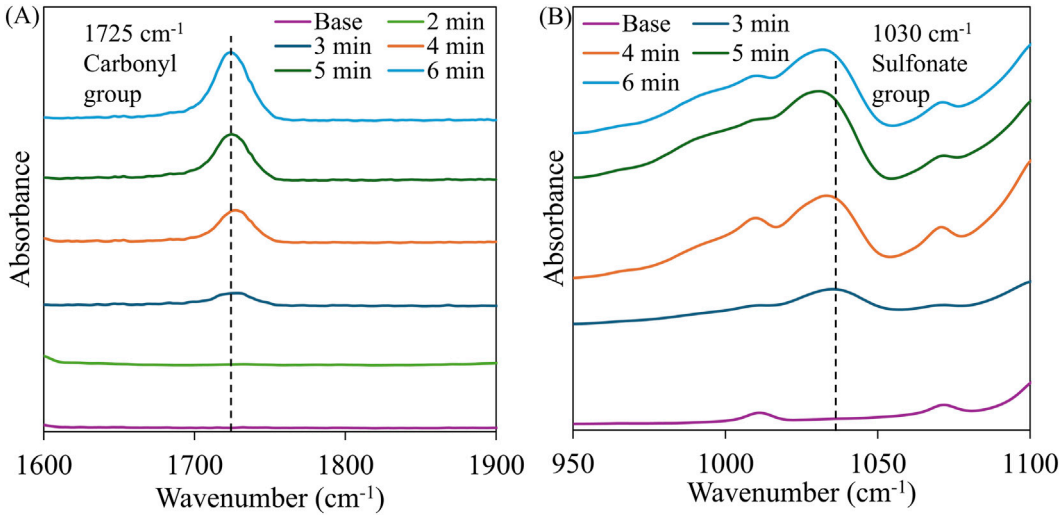

FIGURE 5
FTIR spectra for membranes with different grafting times. **(A)** shows the carbonyl group at 1725 cm^{-1} and **(B)** shows the sulfonate group at 1030 cm^{-1}.

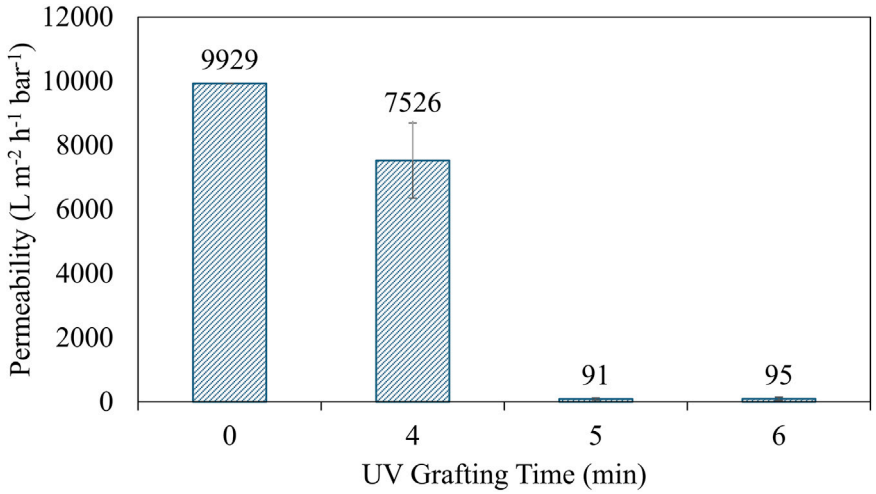

FIGURE 6
DI water permeability measurements for membranes with increasing GMA grafting time.

very low DOG and longer times led to very low permeabilities. Figure 6 indicates very similar permeabilities for 5 and 6 min grafting times. These permeabilities were similar to those obtained for UF membranes. However, Figure 3B indicated that the DOG is higher for 6-min grafting. Thus the static capacity for 6 min grafting was also determined as the required pressure would be similar to current UF membranes. A control experiment using the base membrane was performed with 5–100 ppm Cu^{2+} in solution, but no adsorption was recorded, confirming that functionalization was responsible for binding.

Maximum adsorption capacities and K (adsorption affinity) values for both membranes were calculated using Equations 5, 6. The values were 111 mg/g and 0.073 L/g, for 4-min grafting 149 mg/g and 0.012 L/g, for 6 min grafting for adsorption capacity and adsorption affinity, respectively. However even after 24 h incubation at a solution concentration of 100 ppm, the 4-min grafted membrane displays a higher amount of copper adsorbed per gram of grafted weight than the 6 min grafted membrane.

All membranes were regenerated and reused for static binding experiments. After static adsorption was completed, the membranes were placed in a 1 M sodium chloride and then equilibrated in DI water. The next higher concentration was then tested. Repeated testing at the same concentration indicated complete regeneration.

3.3 Filtration experiments and dynamic binding

Filtration experiments were performed using membranes with 4 min grating only as 6 min grafting led to much higher feed

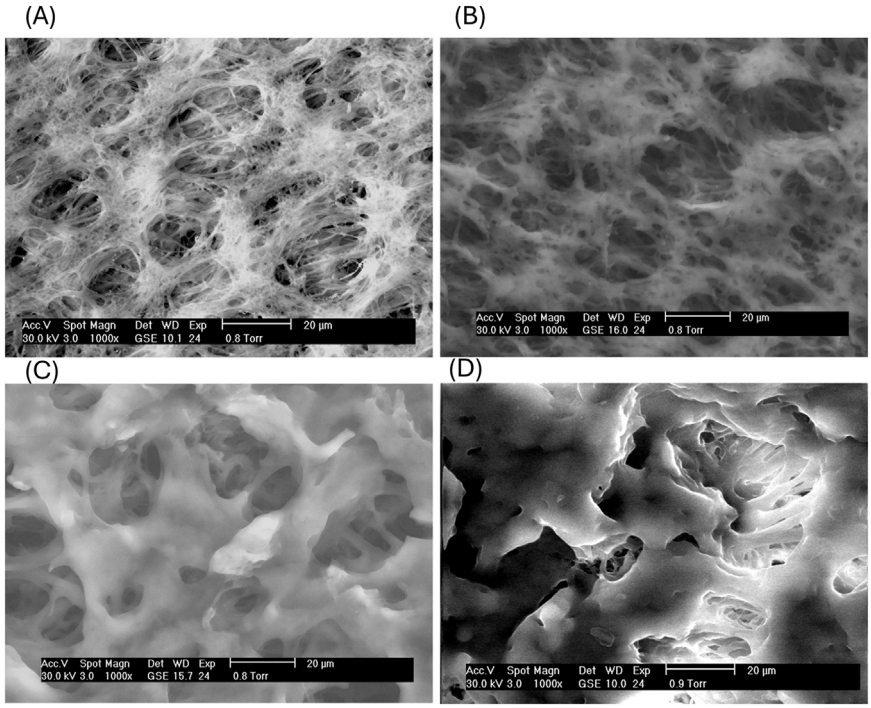

FIGURE 7
SEM images of **(A)** unmodified, **(B)** 4 min grafting **(C)** the 5 min grafting **(D)** 6 min grafting.

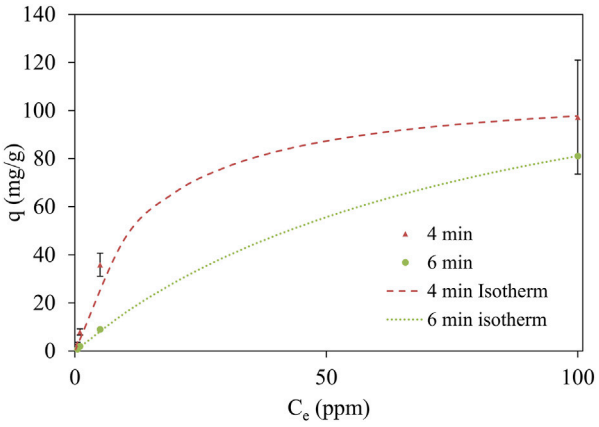

FIGURE 8
Equilibrium adsorption of copper for 4 and 6-min grafted membranes.

pressures for a flux of 135 Lm^{-2} h^{-1}. Filtration was performed at both 1 ppm and 10 ppm concentrations of copper in the feed. The flow rate in these experiments was fixed at 4 mL/min leading to a flux of 135 Lm^{-2} h^{-1}. The resulting breakthrough curves are presented in Figure 9A. Breakthrough was defined as the throughput at which C/C_0 (concentration in permeate divided by concentration in feed) was greater 0.05. In order to ensure that Cu^{2+} ions are being adsorbed by a chemical ion exchange process and not by non-specific physical adsorption, control experiments were conducted where the base PES membranes were incubated with 5–100 ppm of Cu^{2+} ions in DI water. Less than 1% of the Cu^{2+} ions were captured, confirming minimal physical adsorption. As can be seen from Figure 9A, breakthrough occurred for a throughput of 90 mL and <10 mL for copper concentrations of 1 and 10 ppm respectively in the feed.

The dynamic capacity was defined as $C/C_0 = 0.7$. Figure 9A gives the variation of C/C_0 with throughput for a feed concentration of 1 and 10 ppm copper. For 10 ppm copper in the feed, C/C_0 reached 0.7 for a throughput of 70 mL. However for 1 ppm copper in the feed, the dynamic binding capacity was not reached. The dynamic binding capacity was calculated to be 64.5 ± 0.6 mg/g. The feed pressure was <0.07 bar confirming low pressure operation. The error bars represent the range of values for duplicate experiments.

Figure 9B gives the variation of C/C_0 with throughput for three membranes in series. The copper concentration in the feed was 10 ppm. The dynamic binding capacity 70.9 mg/g. Since the capacity is given in terms of mg copper adsorbed per grafted weight the values are similar indicating the process, like all membrane processes is linearly scalable. The pressure for this configuration was <0.15 bar.

As can be seen the static capacity is higher than the dynamic capacity and the time for static binding is greater for membranes with grafting times of 6 min compared to 4 min (see Figure 8). This is due to diffusional resistance in the nanolayer.

4 Discussion

A trade-off exists between capacity and permeability when functionalizing membranes through post-casting modification since the grafting process leads to an additional resistance to

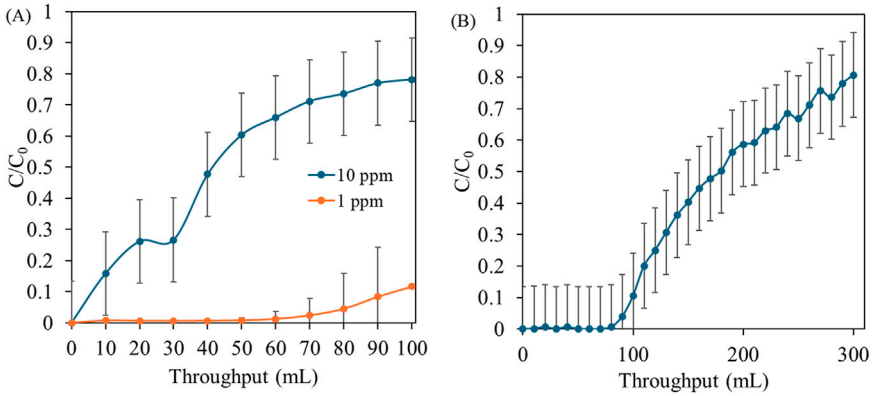

FIGURE 9
Breakthrough curves for **(A)** single membrane with 1 and 10 ppm Cu^{2+} in the feed and **(B)** three membranes in series with 10 ppm Cu^{2+} in the feed.

permeate flow. This is due not only to grafting an additional polymer layer on the membrane surface but also in the membrane pores (Car et al., 2018). Thus, higher DOG will lead to lower permeate fluxes or higher-pressure operation. The FTIR spectra (Figure 5) indicate that a greater DOG leads to more pronounced carbonyl and sulfonate peaks indicating a greater abundance of these groups on the membrane surface. The SEM images also indicate that increasing the grafting time leads to more grafted material on the membrane surface and in the pores. This buildup corresponds with the observed decline in permeability.

Figure 8 gives static adsorption data for copper concentrations up to 100 ppm. In practical application the copper concentration in the wastewater can be over 100 ppm. Here adsorption from solutions containing up to 100 ppm were tested since it is rare to have higher concentrations (Liu et al., 2023). The results in Figure 8 indicate that even though the calculated capacity for the 6-min grafted membrane is higher than for 4-min grafting, even after 24 h incubation for concentrations of up to 100 ppm, the amount adsorbed per grafted weight for the 4 min membrane is still higher. This suggests that at high DOG, many adsorption sites could be sterically hindered or inside the pores that are no longer accessible (Car et al., 2018).

The adsorptive membranes developed here are compared to other adsorptive membranes in Table 1 which gives Q, the maximum static capacity and K the adsorption affinity for copper concentrations that leads to 50% loading. The data in Table 1 indicates that the membranes developed here provide similar capacities. In addition operating pressures are also low. UV initiated polymerization is routinely used industrially as it fast and efficient. The ligands grafted here are not specific. Thus they are better suited for removal of a variety of heavy metals rather than a specific metal ion (Singh et al., 2024). Further, establishment of a full-scale water treatment plant in many rural areas is not feasible and the fact that these membranes are capable of low-pressure operation offers the potential to create a new treatment system capable of addressing a growing issue as manufacturing activity continues to increase.

Earlier studies indicate the importance of comparing breakthrough curves using generalized coordinates in order to determine the effect of the various operating variables (Han et al., 2006; Charcosset et al., 1995). One such basis uses a dimensionless throughput parameter T where

$$T = \frac{(C_0 + 1/K)Q_f t}{Q_m V_m} \tag{7}$$

In Equation 7, where Q_f is the permeate flow rate through the membrane, V_m is the total membrane volume including solid matrix and void space, and t is the run time. In fact T is the ratio of the mass of copper in the feed ($Q_f C_0 t$) to the mass of copper the membrane can adsorb at equilibrium. Figure 10 shows the variation of C/C_0 versus T for the data shown in Figure 9A.

Figure 9A indicates that self-similar behavior is not observed. Rather for a 10-fold difference in feed concentration the residual Cu^{2+} concentration in the permeate is much higher at the same T value for the 10 ppm feed stream. Consequently, diffusion-reaction resistance within the grafted nanostructure is significant, which is supported by the fact that the static capacity is greater than the dynamic capacity. Optimizing the three dimensional structure of the grafted nanolayer will be important to minimize diffusional resistances through the nanolayer.

The results obtained here for one and three membranes in series suggest that the membranes are linearly scalable. There is limited information available regarding the dynamic binding capacity for metal adsorption with membrane adsorbers. Literature relevant to this work reports dynamic binding capacities of 1.77 ± 0.04 g La^{3+}/g membrane using a lysine-grafted PES membrane (Yu et al., 2020), approximately 10 mg Cu^{2+}/g membrane using a chitosan-based membrane adsorber (Wang et al., 2016), and 6.25 mg/g using a PES mixed matrix membrane (Zheng et al., 2014). Membranes in this work exceed these binding capacities. The advantages of the membranes developed here is that they could lead to effective treatment options for water contaminated with mixtures of heavy metals.

Membrane-in-series experiments highlight the ability to easily increase the surface area. These experiments also confirmed the ability of the membrane module to extend the treatment volume where the membranes could provide removal of copper from the feed below the EPA limit of 1.3 ppm. It is also crucial that stacking the membranes in series did not further increase the operating pressure significantly. This suggests that further increasing the active

TABLE 1 Q and K terms calculated for membranes in this work and comparison to literature.

Adsorbent	Membrane material	Q (mg g^{-1})	K (L mg^{-1})	Ref
Sulfonic acid	4-min grafted PES	111	0.07	This work
Sulfonic acid	6-min grafted PES	149	0.01	This work
Amine	PVDF-poly (GMA)	1.65	0.009	Sepesy et al. (2022)
Amine	Polysulfone-*block*-poly (acrylic acid)	50.8	0.001	Zhang et al. (2018)
Amine	Electrospun polyacrylonitrile	250	0.0059	Shao et al. (2021)
Chitosan	Chitosan + glutaraldehyde	87.469	0.785	Wang et al. (2016)
Chitosan	Nylon	10.794		He et al. (2008)
Chitosan + Amine	Chitosan/polyvinyl alcohol/carbon nanotube mixed matrix membrane	35		Salehi et al. (2013)
Resin	PES mixed matrix membrane	161.29		Zheng et al. (2014)
Poly (2-aminoethyl methacrylate)	Polypropylene	90.3	0.03	Farjadian et al. (2015)

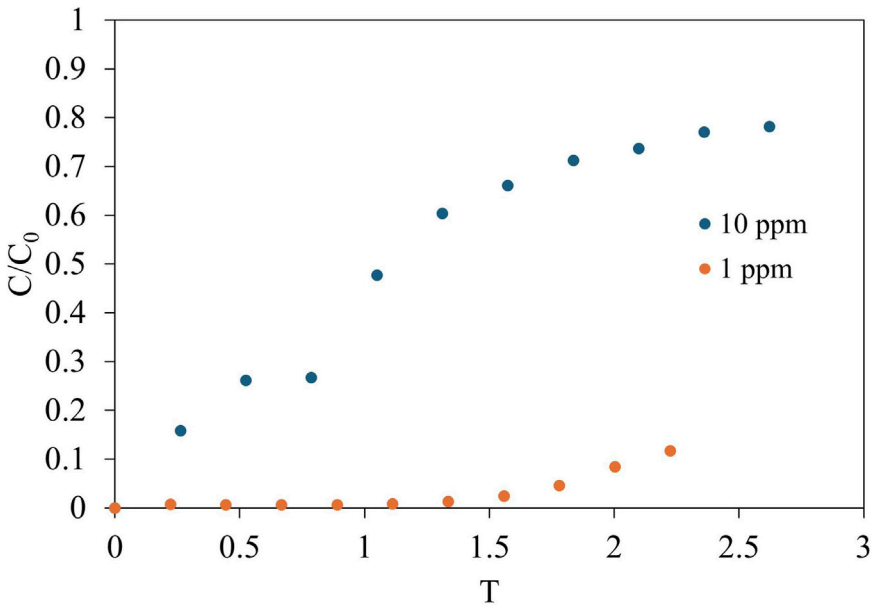

FIGURE 10
Variation of C/Co with T for feed concentrations for 1 and 10 ppm Cu^{2+}.

area and stacking more membranes in series is possible without compromising the ability to operate without significant infrastructure. This allows for the ability to increase the active membrane area to further increase the throughput while maintaining the desired footprint. Scaling the membrane area based on the results in this work, to the size of current commercial systems (37 m^2 (AXEON Water, 2024)), would result in a throughput of approximately 64 L at 100 ppm and as high as approximately 3000 L for treating drinking water with lower concentrations around 2 ppm (Zhang et al., 2020). In such a system, competing ions need to be considered given the nonspecific nature of the adsorption mechanism. Zhang et al. (2020) indicate that copper represents approximately 60% of the heavy metal ions present, which would decrease the treatment volume to 1800 L. The actual value would likely be lower given the presence of other cations not reported, however a potential solution could be to combine this with a nanofiltration or similar process capable of isolating these divalent ions from their monovalent competitors. The results highlight the potential of the membranes reported in this work to be scaled into a system capable of capturing heavy metals from water in a portable configuration that does not currently exist.

Literature reports on metal adsorption mechanisms suggest it is reasonable to assume that these metals of similar valency would have similar adsorption capacities to the capacity of copper reported in this work (Jasim and Ajjam, 2024; Mohammed and Mahmood, 2023). Previous studies also demonstrate the ability of sulfonic acid groups to capture a variety of different heavy metal ions through ion

exchange interactions. Heavy metals such as Ag (I), Hg (II), Cd (II), Zn (II), Pb (II), and Cr (III) are successfully captured using sulfonic acid ligands (Rivas and Ruf, 2003). Similar performance was observed for each metal which can be attributed to nonspecific ion exchange removal mechanism. Qu et al. investigated the removal of Pb (II), Cd (II), and Cu (II) using sulfonic acid ligands at higher initial metal concentrations of 1000 ppm. They found that at these high concentrations Pb and Cd were more efficiently captured than Cu (Qu et al., 2012). This is likely related to ionic radii of these ions given the ions must first hydrolyze before they are able to undergo the ion exchange adsorption process (Eldridge et al., 2015). While the focus of this work was on controlling the grafting reaction future work will explore removal of these ions as well as scaling the system to a practical size.

For the PES membrane tested here, higher DOG was not investigated for three main reasons. Very long grafting times would result in greater UV exposure which was found to lead to increased permeate fluxes and reduced mechanical stability due to membrane damage. Further as indicated in Figure 6, higher DOG led to reduced permeability which would adversely affect low pressure operation. In addition a high density grafted nanostructure leads to increased diffusional resistances to metal ion adsorption as indicated by Figure 8. Here 0.22 μm pore size PES membranes were investigated. However use of larger pore size membranes, e.g., 0.4 μm, may enable grafting of a thicker three dimensionally tailored nanolayer. In this way the ionic capacity can be maximized while still maintaining low pressure operation and minimal diffusional resistance for solute adsorption within the nanostructure.

Grafting conditions will affect the properties of the grafted nanolayer. Wang et al. (2009) provide a detailed analysis of how reaction conditions may be tailored to optimize static and dynamic capacity. While higher reaction temperatures may lead to higher rates of grafting, it is essential that the elevated reaction temperature does not degrade the PES membrane. It is difficult to independently control GMA density and length using the photo-initiated radical polymerization method used here. Higher initiator densities will lead to higher grafted chain densities. In this work grafting is based on the photosensitivity of the poly (aryl sulfone) backbone, which undergoes photolysis when exposed to UV radiation. The major advantage of this method is that no initiator is required. However the number of initiation sites is fixed by the polymer backbone. Further, over irradiation will lead to weakened membranes. Higher GMA concentrations will tend to lead to longer chains for a given grafting time and temperature though chain density will also be affected.

Earlier studies indicate that maximizing the number of ion exchange sites will not maximize the dynamic capacity (Wickramasinghe et al., 2006). Long GMA chains will lead to steric hindrance effects where access to adsorption sites deep within the nanolayer will require significant diffusion times for metal ions. In addition a thicker nanolayer can also result in reduced permeability. The results obtained here are in keeping with these observations. Figure 6 indicates that longer polymerization times lead to lower permeability while Figure 8 indicates that longer grafting times lead to slower static adsorption rates due to increased diffusional resistance. As indicated by previous investigators by optimizing the three dimensional nanolayer by including a spacer species between GMA monomers or by grafting branched polymer chains from the membrane surface higher dynamic capacities (Wang et al., 2009; Wickramasinghe et al., 2006) can result.

The effect of fouling using real wastewater was not investigated here. Our initial application would be to use the membrane adsorber as a final polishing step, e.g., to remove hardness from water. For this application no significant fouling is expected. On the other hand, for other applications fouling is likely. Our future work will investigate the effect of fouling, e.g., by using feed streams that contain natural organic matter (NOM).

5 Conclusion

This work reports the successful development of membrane adsorbers capable of copper capture at low pressure through photo-initiated radical polymerization and subsequent sulfonic acid functionalization. By investigating a range of modification conditions, optimal conditions to increase functionality without compromising low-pressure operation were determined. Membranes functionalized with 4 min grafting time displayed static and dynamic capacities of 111 mg/g and 64.05 ± 0.6 mg/g, respectively. Membrane in series experiments highlighted liner scalability enabling increased throughput while maintaining low-pressure operation. The linear scalability and low-pressure operation demonstrated in this work could enable the possibility of designing technologies capable of capturing heavy metals in places where creation of full-scale water treatment plants is not feasible.

Data availability statement

The raw data supporting the conclusions of this article will be made available by the authors, without undue reservation.

Author contributions

TM: Conceptualization, Data curation, Formal Analysis, Investigation, Methodology, Project administration, Resources, Supervision, Validation, Visualization, Writing – original draft, Writing – review and editing. CW: Conceptualization, Data curation, Formal Analysis, Investigation, Resources, Validation, Visualization, Writing – original draft. SW: Conceptualization, Funding acquisition, Methodology, Project administration, Supervision, Writing – review and editing. JH: Conceptualization, Funding acquisition, Methodology, Project administration, Supervision, Writing – review and editing.

Funding

The author(s) declared that financial support was received for this work and/or its publication. Funding for this project was provided by the University of Arkansas Chancellors Innovation Fund, the University of Arkansas Honors College, the Ralph E. Martin Department of Chemical Engineering, and Lifeplus.

Conflict of interest

The author(s) declared that this work was conducted in the absence of any commercial or financial relationships that could be construed as a potential conflict of interest.

The author SW declared that they were an editorial board member of Frontiers, at the time of submission. This had no impact on the peer review process and the final decision.

Generative AI statement

The author(s) declared that generative AI was not used in the creation of this manuscript.

Any alternative text (alt text) provided alongside figures in this article has been generated by Frontiers with the support of artificial intelligence and reasonable efforts have been made to ensure accuracy, including review by the authors wherever possible. If you identify any issues, please contact us.

Publisher's note

All claims expressed in this article are solely those of the authors and do not necessarily represent those of their affiliated organizations, or those of the publisher, the editors and the reviewers. Any product that may be evaluated in this article, or claim that may be made by its manufacturer, is not guaranteed or endorsed by the publisher.

References

Agarwal, A., Upadhyay, U., Sreedhar, I., Singh, S. A., and Patel, C. M. (2020). A review on valorization of biomass in heavy metal removal from wastewater. *J. Water Process Eng.* 38, 101602. doi:10.1016/J.JWPE.2020.101602

Akale, S., and Shaikh, I. N. (2024). Mixed-matrix membrane designed with water channels and sieving effect for effective removal of heavy metals. *Environ. Nanotechnol. Monit. Manag.* 22, 100985. doi:10.1016/J.ENMM.2024.100985

Albqmi, M., Frontistis, Z., Raji, Z., Karim, A., Karam, A., and Khalloufi, S. (2023). Adsorption of heavy metals: mechanisms, kinetics, and applications of various adsorbents in wastewater remediation—A review. *Waste.* 1 (3), 775–805. doi:10.3390/WASTE1030046

AXEON Water (2024). Commercial RO membrane selection guide. Available online at: https://www.axeonwater.com/blog/commercial-ro-membrane-selection-guide/ (Accessed October 6, 2025).

Barakat, M. A., and Schmidt, E. (2010). Polymer-enhanced ultrafiltration process for heavy metals removal from industrial wastewater. *Desalination* 256 (1-3), 90–93. doi:10.1016/J.DESAL.2010.02.008

Bondar, Y., Kim, H. J., Yoon, S. H., and Lim, Y. J. (2004). Synthesis of cation-exchange adsorbent for anchoring metal ions by modification of Poly(Glycidyl methacrylate) chains grafted onto polypropylene fabric. *React. Funct. Polym.* 58 (1), 43–51. doi:10.1016/J.REACTFUNCTPOLYM.2003.11.006

Carter, B. M., Sengupta, A., Qian, X., Ulbricht, M., and Wickramasinghe, S. R. (2018). Controlling external versus internal pore modification of ultrafiltration membranes using surface-initiated AGET-ATRP. *J. Membr. Sci.* 554, 109–116. doi:10.1016/j.memsci.2018.02.066

Charcosset, C., Su, Z., Karoor, S., Daun, G., and Colton, C. K. (1995). Protein A immunoaffinity hollow fiber membranes for immunoglobulin G purification: experimental characterization. *Biotechnol. Bioeng.* 48 (4), 415–427. doi:10.1002/bit.260480414

Chitpong, N., and Husson, S. M. (2017a). Polyacid functionalized cellulose nanofiber membranes for removal of heavy metals from impaired waters. *J. Memb. Sci.* 523 (1), 418–429. doi:10.1016/J.MEMSCI.2016.10.020.0

Chitpong, N., and Husson, S. M. (2017b). High-capacity, nanofiber-based ion-exchange membranes for the selective recovery of heavy metals from impaired waters. *Sep. Purif. Technol.* 179, 94–103. doi:10.1016/J.SEPPUR.2017.02.009

Eldridge, D. S., Crawford, R. J., and Harding, I. H. (2015). The role of metal ion-ligand interactions during divalent metal ion adsorption. *J. Colloid Interface Sci.* 454, 20–26. doi:10.1016/j.jcis.2015.04.056

Ennigrou, D. J., Gzara, L., Romdhane, M. R., and Dhahbi, M. (2009). Cadmium removal from aqueous solutions by polyelectrolyte enhanced ultrafiltration. *Desalination* 246 (1-3), 363–369. doi:10.1016/j.desal.2008.04.053

Escamilla, P., Monteleone, M., Percoco, R. M., Mastropietro, T. F., Longo, M., Esposito, E., et al. (2024). BioMOF@PAN mixed matrix membranes as fast and efficient adsorbing materials for multiple heavy metals' removal. *ACS Appl. Mater Interfaces* 16 (38), 51182–51194. doi:10.1021/acsami.4c12363

Farjadian, F., Schwark, S., and Ulbricht, M. (2015). Novel functionalization of porous polypropylene microfiltration membranes: via grafted Poly(Aminoethyl methacrylate) anchored schiff bases toward membrane adsorbers for metal ions. *Polym. Chem.* 6 (9), 1584–1593. doi:10.1039/C4PY01521E

Fraser, A. C., Yankey, J., Coronell, O., and Dingemans, T. J. (2022). A sulfonated all-aromatic polyamide for heavy metal capture: a model study with Pb(II). *ACS Appl. Polym. Mater* 5 (1), 856–865. doi:10.1021/ACSAPM.2C01796

Garcia-Chirino, J., Van Eygen, G., Bathia, M., Liu, R., Guo, W., Volodine, A., et al. (2025). Sustainable fabrication of mixed matrix membranes using oxycut powder from steel waste for efficient heavy metal removal. *J. Memb. Sci.* 723, 123956. doi:10.1016/J.MEMSCI.2025.123956

Han, B., Carvalho, W., Canilha, L., da Silva, S. S., Almeida, e, Silva, J. B., et al. (2006). Adsorptive membranes vs. rresins for acetic acid removal from biomass hydrolysates. *Desalination* 193 (1–3), 361–366. doi:10.1016/j.desal.2005.07.052

He, Z. Y., Nie, H. L., Branford-White, C., Zhu, L. M., Zhou, Y. T., and Zheng, Y. (2008). Removal of Cu2+ from aqueous solution by adsorption onto a novel activated nylon-based membrane. *Bioresour. Technol.* 99 (17), 7954–7958. doi:10.1016/J.BIORTECH.2008.04.001

Huang, J. H., Zeng, G. M., Zhou, C. F., Li, X., Shi, L. J., and He, S. B. (2010). Adsorption of surfactant micelles and Cd^{2+}/Zn^{2+} in micellar-enhanced ultrafiltration. *J. Hazard Mater* 183 (1-3), 287–293. doi:10.1016/J.JHAZMAT.2010.07.022

Jaishankar, M., Tseten, T., Anbalagan, N., Mathew, B. B., and Beeregowda, K. N. (2014). Toxicity, mechanism and health effects of some heavy metals. *Interdiscip. Toxicol.* 7 (2), 60–72. doi:10.2478/INTOX-2014-0009

Jasim, A. Q., and Ajjam, A. K. (2024). Removal of heavy metal ions from wastewater using ion exchange resin in a batch process with kinetic isotherm. *S Afr. J. Chem. Eng.* 49, 43–54. doi:10.1016/j.sajce.2024.04.002

Johnson, L., and Duval, C. E. (2025). Rare-earth element adsorption to membranes functionalized with Lanmodulin-Derived peptides. *Langmuir* 41 (14), 9581–9589. doi:10.1021/ACS.LANGMUIR.5C00969

Khodabakhshi, M. R., and Goodarzi, V. (2021). Preparing and analysis an innovative membrane based on polyethersulfone/sulfonated polyethersulfone/organically modified nanoclay: ability to heavy metal removal. *Mater Today Commun.* 26, 101957. doi:10.1016/J.MTCOMM.2020.101957

Liang, R., and Zou, H. (2020). Removal of aqueous Hg(II) by thiol-functionalized nonporous silica microspheres prepared by one-step sol–gel method. *RSC Adv.* 10 (31), 18534–18542. doi:10.1039/d0ra02759f

Liu, Y., Wang, H., Cui, Y., and Chen, N. (2023). Removal of copper ions from wastewater: a review. *Int. J. Environ. Res. Public Health* 20 (5), 3885. doi:10.3390/ijerph20053885

Mohammed, A. A., and Mahmood, H. S. (2023). Removal of Cu^{2+}, Pb^{2+}, and Ni^{2+} ions from simulated waste water by ion exchange method on zeolite and purolite C105 resin. *J. Eng.* 19 (10), 1327–1340. doi:10.31026/j.eng.2013.10.10

Mukherjee, R., Bhunia, P., and De, S. (2016). Impact of graphene oxide on removal of heavy metals using mixed matrix membrane. *Chem. Eng. J.* 292, 284–297. doi:10.1016/J.CEJ.2016.02.015

Neolaka, Y. A., Riwu, A. A., Aigbe, U. O., Ukhurebor, K. E., Onyancha, R. B., Darmokoesoemo, H., et al. (2023). Potential of activated carbon from various sources as a low-cost adsorbent to remove heavy metals and synthetic dyes. *Results Chem.* 5, 100711. doi:10.1016/J.RECHEM.2022.100711

Nompumelelo, K. S., Edward, N. N., Muthumuni, M., Moloko, M., and Makwena, M. J. (2023). Fabrication, modification, and mechanism of nanofiltration membranes for the removal of heavy metal ions from wastewater. *ChemistrySelect* 8 (33), e202300741. doi:10.1002/SLCT.202300741

Ozaki, H., Sharma, K., and Saktaywin, W. (2002). Performance of an ultra-low-pressure reverse osmosis membrane (ULPROM) for separating heavy metal: effects of interference parameters. *Desalination* 144 (1-3), 287–294. doi:10.1016/S0011-9164(02)00329-6

Pei, X., Gan, L., Tong, Z., Gao, H., Meng, S., Zhang, W., et al. (2021). Robust cellulose-based composite adsorption membrane for heavy metal removal. *J. Hazard Mater* 406, 124746. doi:10.1016/J.JHAZMAT.2020.124746

Petrinic, I., Korenak, J., Povodnik, D., and Hélix-Nielsen, C. A. (2015). Feasibility study of Ultrafiltration/reverse osmosis (UF/RO)-Based wastewater treatment and reuse in the metal finishing industry. *J. Clean. Prod.* 101, 292–300. doi:10.1016/J.JCLEPRO.2015.04.022

Qu, Q., Gu, Q., Gu, Z., Shen, Y., Wang, C., and Hu, X. (2012). Efficient removal of heavy metal from aqueous solution by sulfonic acid functionalized nonporous silica microspheres. *Colloids Surf. A Physicochem Eng. Asp.* 415, 41–46. doi:10.1016/J.COLSURFA.2012.08.059

Razzak, S. A., Faruque, M. O., Alsheikh, Z., Alsheikhmohama, L., Alkuroud, D., Alfayez, A., et al. (2022). A comprehensive review on conventional and biological-driven heavy metals removal from industrial wastewater. *Env. Adv.* 7, 100168. doi:10.1016/J.ENVADV.2022.100168

Rivas, B. L., and Ruf, B. (2003). Preparation and metal ion adsorption properties of the resin containing sulfonic acid groups. *J. Appl. Polym. Sci.* 88 (5), 1230–1235. doi:10.1002/app.11784

Salehi, E., Madaeni, S. S., Rajabi, L., Derakhshan, A. A., Daraei, S., and Vatanpour, V. (2013). Static and dynamic adsorption of copper ions on Chitosan/polyvinyl alcohol thin adsorptive membranes: combined effect of polyethylene glycol and aminated multi-walled carbon nanotubes. *Chem. Eng. J.* 215-216 (215–216), 791–801. doi:10.1016/J.CEJ.2012.11.071

Sepesy, M., Fugate, B., and Duval, C. E. (2022). Amine-functionalized membrane adsorbers to purify copper from acidic solutions. *ACS Appl. Polym. Mater* 4 (5), 3034–3044. doi:10.1021/ACSAPM.1C01512

Shao, H., Yin, D., Li, D., Ma, Q., Yu, W., and Dong, X. (2021). Simultaneous visual detection and removal of Cu^{2+} with electrospun self-supporting flexible amidated polyacrylonitrile/branched polyethyleneimine nanofiber membranes. *ACS Appl. Mater Interfaces* 13 (41), 49288–49300. doi:10.1021/ACSAMI.1C13722.6

Singh, V., Ahmed, G., Vedika, S., Kumar, P., Chaturvedi, S. K., Rai, S. N., et al. (2024). Toxic heavy metal ions contamination in water and their sustainable reduction by eco-friendly methods: isotherms, thermodynamics and kinetics study. *Sci. Rep.* 14, 1–13. doi:10.1038/S41598-024-58061-3

Sokker, H. H., Badawy, S. M., Zayed, E. M., Eldien, F. A., and Farag, A. M. (2009). Radiation-induced grafting of glycidyl methacrylate onto cotton fabric waste and its modification for anchoring hazardous wastes from their solutions. *J. Hazard Mater* 168 (1), 137–144. doi:10.1016/J.JHAZMAT.2009.02.039

Soon, W. L., Peydayesh, M., Bui, M. H., Perrin, Q. M., Mezzenga, R., and Miserez, A. (2024). Copper decontamination using feather keratin amyloid-carbon hybrid membranes. *ACS ES&T Water* 4 (1), 309–313. doi:10.1021/acsestwater.3c00694

U.S. Environmental Protection Agency (2025). *Lead and copper rule*. Washington, DC: U.S. Environmental Protection Agency. Available online at: https://www.epa.gov/dwreginfo/lead-and-copper-rule.

Vatanpour, V., Mehrabi, M., Masteri-Farahani, M., Behroozi, A. H., Niakan, M., and Koyuncu, I. (2022). Sulfonic acid functionalized dendrimer-grafted cellulose as a charge and hydrophilic modifier of cellulose acetate membranes in removal of inorganic and organic pollutants. *J. Water Process Eng.* 50, 103307. doi:10.1016/J.JWPE.2022.103307

Wang, J., Faber, R., and Ulbricht, M. (2009). Influence of pore structure and architecture of photo-initiated functional layers on separation performance of cellulose-based microporous membrane absorbers. *J. Chromatogr. A* 1216 (36), 6490–6501. doi:10.1016/j.chroma.2009.07.030

Wang, X., Li, Y., Li, H., and Yang, C. (2016). Chitosan membrane adsorber for low concentration copper ion removal. *Carbohydr. Polym.* 146, 274–281. doi:10.1016/J.CARBPOL.2016.03.055

Wanjiya, M., Zhang, J. C., Wu, B., Yin, M. J., and An, Q. F. (2024). Nanofiltration membranes for sustainable removal of heavy metal ions from polluted water: a review and future perspective. *Desalination* 578, 117441. doi:10.1016/J.DESAL.2024.117441

Wickramasinghe, S. R., Han, B., Carlson, J. O., Teske, C., Hubbuch, J., and Ulbricht, M. (2006). Characterizing solute binding to macroporous ion exchange membrane adsorbers using confocal laser scanning microscopy. *J. Membr. Sci.* 281 (1-2), 609–618. doi:10.1016/j.memsci.2006.04.034

Xiang, H., Min, X., Tang, C. J., Sillanpää, M., and Zhao, F. (2022). Recent advances in membrane filtration for heavy metal removal from wastewater: a mini review. *J. Water Process Eng.* 49, 103023. doi:10.1016/J.JWPE.2022.103023

Yu, M., Renner, J. N., and Duval, C. E. (2020). A lysine-modified polyethersulfone (PES) membrane for the recovery of lanthanides. *Front. Chem.* 8, 8. doi:10.3389/FCHEM.2020.00512

Yune, P. S., Kilduff, J. E., and Belfort, G. (2012). Searching for novel membrane chemistries: producing a large library from a single graft monomer at high throughput. *J. Memb. Sci.* 390-391, 390–391. doi:10.1016/J.MEMSCI.2011.10.048

Zhang, Y., Vallin, J. R., Sahoo, J. K., Gao, F., Boudouris, B. W., Webber, M. J., et al. (2018). High-affinity detection and capture of heavy metal contaminants using block polymer composite membranes. *ACS Cent. Sci.* 4 (12), 1697–1707. doi:10.1021/ACSCENTSCI.8B00690

Zhang, J., Wang, G., Zhang, Y., Zhao, F., Zhu, Y., Cui, X., et al. (2020). Pollution, sources and environmental risk assessment of heavy metals in the surface AMD water, sediments and surface soils around unexploited rona Cu deposit, Tibet, China. *Chemosphere* 248, 125988. doi:10.1016/j.chemosphere.2020.125988

Zheng, G., Ye, H., Zhang, Y., Li, H., Lin, L., and Ding, X. (2014). Removal of heavy metal in drinking water resource with cation-exchange resins (type 110-H) mixed PES membrane adsorbents. *J. Hazard Toxic. Radioact. Waste* 19 (1), 04014026. doi:10.1061/(ASCE)HZ.2153-5515.0000229